The Research and Development of Dissolved Oxygen Chip Sensor for Aquaculture Fishery Industry

Wen-Cheng Kuo[1*], Wei-Chih Lan[1], Kuan-Hung Sun[2]

[1]Department of Mechanical and Automation Engineering, National Kaohsiung First University of Science and Technology
[2]Department of Information Management, Fortune Institute of Technology
E-mail: rkuo@nkfust.edu.tw

Abstract - The inland aquaculture production is 30% of the total fishery production in Taiwan. However, the dissolved oxygen in the acquaculture water is likely to change because of external factors causing the aquacultural products dying. In order to reduce the loss of aquaculture production and ensure successful aquzcultural products, a monitoring system for the dissolved oxygen in the aquaculture water is required. A water quality dissolved oxygen sensor is developed in this study. Based on the principles of electrochemistry, having silicon wafer as the substrate, and depositing metal on silicon wafers as the electrode, the solid electrolyte is mixed and coated on the metal sensing electrode. Finally, a layer of waterproof and permeable film is coated on the solid electrolyte to complete the production of the dissolved oxygen chip sensor. The developed chip is placed in the solution with water temperature 26 ℃ and stirring speed 750 rpm and measured the dissolved oxygen with 8 ppm, 6 ppm, 4 ppm, 2 ppm, and 0 ppm so as to test the performance of the dissolved oxygen chip sensor. Based on the results, the measurements of the solution with different dissolved oxygen are drawn the calibration curves of electric current and water dissolved oxygen with Cyclic voltammetry. According to the curves, the sensitivity of the dissolved oxygen chip sensor is 0.278 μA/ppm, the linear relationship R^2 0.9531, and the response time 15 sec.

Keywords: electrochemistry, dissolved oxygen, solid electrolyte, aquaculture

I. INTRODUCTION

Surrounded by seas, the main island of Taiwan is 395 km long and the coastline is up to 1,000 km long. About 88 islands, including Penghu Isl ands, Lamay Island, Green Island, Orchid Island, Keelsung Islet, Guishan Island, Pengjia Islet and so fort h, are contained. When the 200 *nm* (about 370 *km*) economic zone is included, the m aritime boundary (about 180,000 *km²*) of Taiwan is far larger than the land territory. Taiwan therefore is an island country with long shore and wide coastl waters. The west ern Taiwan presents the ease and flat land with Kuroshio current, ocean current, and monsoon; while the eastern area i s the rendezvous of col d and warm currents that it is the favorable habitat for shellfish, fish, and shrimps.

Unfortunately, the marine creatures and the fishery production are no longer as abundant as they used to be that the fishery resources are getting deficient. The major factors include habitat destruction, environmental pollution, over-catching, importing alien species, and global climate change. Consequently, the inland aquaculture fishery industry has been rapidly developed to promptly increase the production of inland aquaculture. In 2009, t he total fishery production in Taiwan and Fujian areas reached 1,089,178 tones with the total output 86 billion NT dollars, which dropped 18.75% of the total fishery production and 6.44% of t he total output in comparison with them in 2008. M oreover, the fishery production of the inland aquaculture was 255,114 tons with the output 27 billion NT dollars in 2009, which was 30% of the total output [1]. Inland aquaculture therefore has become the key lifeline in fishery industry.

With the increase of population, the demand for protein from chickens, ducks, and fi sh is increasing in Taiwan that aquatic fish, in addtion to terrestrial animals, has become an important source of ani mal protein. Moreover, consumers present higher requirements on the quality that aquatic food has been changed from salted, freshly frozen, to live. The taste of dead fi sh is no l onger satisfactory. More and more seafood restaurants have em erged on st reets in Taiwan, in which live fish directly deliverd from the place of origin has become the attraction of fresh delicacies for custom ers. In this case, when t he demand is enhancing, the freshness of seafood has been em phasized by gluttons and groumets. It has become critical to understand the living conditions of seafood so as to ensure the growth of fish and shrimps.

Eels, fish, and shrimps, as th e major cultivation of the inland aquaculture fishery in Taiwan, are densely cultivated to promote the production. However, in order to enhance the survival of aquatic fish and reduce t he loss of cost, water quality has become a key factor for aquaculture. As th e water body of a fish farm is much less than lakes and ocean, it is rather difficult to maintain the stability of water quality. Eels, fish, and shrimps are co nsidered sensitive to water quality that the temporarily poor water quality , such as dissolved oxygen reduction, PH val ue change, and t he sudden change of wat er temperature or sal inity, could reduce the energy of the cultivated fish and shrimps or even cause their death and directly result in the loss of aquculture businesses. For this reason, taking care o f water q uality is considered as important as looking after the aquatic fish and shrimps. Stirring and pum ping are t he most common methods to increase the dissolved oxygen in Taiwan at present. In terms of water quality monitoring, the dissolved oxygen is a key factor for aquatic creatures. The solubility of oxygen in water would change with temperature and the partial pressure of oxygen in the atmosphere, while the water dissolved oxygen would change with the temperature and salinity in water, the atmospheric pressure on the surface of water, the decomposition of organic compounds, and the consumption of organisms. Corresponding to Henry's law [2]

$$[O_2] = P_{O_2} \times K_H \qquad (1)$$

where $[O_2]$ is the balance concentration of oxygen in the solution,

P_{O_2} the partial pressure of oxygen, and

K_H the Henry constant.

K_H would change with temperature so that the higher temperature is, lower K_H appears and the lower temperature is, the higher K_H presents. In this case, when the water temperature is higher in summer, the water dissolved oxygen is reduced; contrarily, when t he water temperature is lower in winter, the water dissolved oxygen is increased. Some fish can merely live in high mountains with high dissolved oxygen. When they are moved to the level ground, they are likely to die because of the reduction of water dissolved oxygen. Moreover, when t he salt concentration is increased, the water dissolved oxygen would relatively be reduced [3][4].

In regard to fish, Table 1 shows the adaptation of fish in the water with different dissolved oxygen [5]. D. R . Raible [6] indicated that water q uality with low dissolved oxygen could reduce the energy and the food intake of fish, but the more dissolved oxygen was, the more food intake of the aquatic fish showed. B . A. Si mco [7] found that the aquatic fish would reduce t he food i ntake when the dissolved oxygen dropped t o 3 mg/l and could stop taking food and merely maintain the functions of circulatory system and nervous sy stem when t he dissolved oxygen dropped to 2 mg/l . He also regarded warm water aquaculture system with the dissolved oxygen more than 5 *ppm* as t he optimal condition for t he growth of fish. Besides, the water quality with abundant dissolved oxygen could offer t he best decomposition efficiency of ammonia and nitrite that, when the dissolved oxygen is lower than 2 *ppm*, the digestion bacteria might stop digesting.

Accordingly, dissolved oxygen, as a pri mary factor in aquatic creatures, is involved with the energy and t he survival of cultivated fish and shrimps. For this reason, it is beneficial for aquaculture fishery to monitor the dissolved oxygen. This study therefore tends to produce a dissolved oxygen sensor for aquaculture fishery industry.

II. PROCESSING METHOD

A. Silicon Wafer Film Deposition

With film deposition to produce t he electrode of t he dissolved oxygen chip sensor , the surface of the silicon wafer was cleaned before film deposition. Using the mixture of peroxide (H_2O_2) and sul furic acid (H_2SO_4), with the proportion of peroxide:sulfuric acid = 1︰3, to wash off the splotch on the surface, the s ilicon wafer was placed in the mixture and agi tated with ultrasound for 5 *min*; deionized water was used to clean the rem ained mixture on the wafer; the deionized water on the wafer was t hen removed with a high-pressure air gun; and finally, the wafer was dried on a hot plate. Since silicon wafers were conductive, a layer of 1 *μm*-thick silica (SiO_2), as th e insulator, was deposited on the surface of the silicon wafer . Furthermore, a layer of 400 *Å*-thick chrome (Cr) was deposited on silica with an E-beam evaporator to increase the a dhesion of aurum (Au). Then, the surface of chrome was deposited 2000 *Å*-thick aurum as a sensing electrode.

B. Photo Mask fabrication

With AutoCAD to draw the masks for positive and negative electrodes required by the sensor, the photo mask was further produced.

C. Lithography Process

Evenly coating the positive photoresist AZ4620 on the silicon wafer with a spin coater, preceding the exposure on the mask aligner with mask#1, and t hen developing the silicon wafer, the photoresist still rem ained on the silicon wafer, as i t was covered by mask#1 and not exposed. Placing the silicon wafer in to the aurum etching fluid, the photoresist on the silicon wafer could be the protector for aurum etching. After the etch ing, acetone was utilized for removing the photoresist on the silicon wafer; isopropyl alcohol was used for increasing the hydrophile of the silicon wafer; and, deionized water was used for washi ng the silicon wafer. Th e process of aurum electrode was then completed. Repeating the above st eps, a spin coater was utilized for evenly coati ng the positive photoresist AZ4620 on the surface of the silicon wafer with com pleted aurum electrode. Mask#2 was used for exposure and development on the mask aligner so as to open a hole on the surface of the silicon wafer for depositing silver electrode. An E-beam evaporator was further utilized for depositing 2000 *Å*-thick silver. With Lift-off technique to remove the photoresist, the silver electrode in the hole would be l eft. The process of silver electrode was therefore completed.

Repeating the above steps, a spin coater was utilized for evenly coating the positive photoresist AZ4620 on the surface of the silicon wafer with complete aurum and silver electrodes. Mask#3 was used for exposure and devel opment on the mask aligner; the aurum and silver electrodes on the silicon wafer was protected by the photoresist. The silicon wafer was further placed in the chrome etching fluid for removing the extra chrome under the aurum and silver electrodes. Making it short between electrodes, acetone was then used for removing the photoresist.

Repeating the above steps, a spin coater was utilizing for evenly coating the positive photoresist AZ4620 on the surface of the silicon wafer with com pleted aurum and silver electrodes. Mask#4 was t hen used for exposure and development on the mask aligner; the silver electrode on the silicon wafer th en completed the hole. The wafer was further placed in silver chloride for several seconds. Finally, acetone was used for rem oving the photoresist. The process of reference electrode was then completed. The process flow chart is shown as Fig. 1.

D. Coating Solid Electrolyte

1) Mixing the Solid Electrolyte

By mixing liquid electrolyte potassium nitrate with gelatin, the potassium nitrate gelatin was generated. Having the mixture with the proportions of 2︰1, 4︰1, and 8︰1 heated to 150 ℃, it was fu lly stirred to have gelatin be entirely dissolved in potassium nitrate. The solid electrolyte with different proportions was further tested the impedance and the conductivity.

2) Testing the Conductivity and the Impedance of Solid Electrolyte

In addition to maintaining the characteristics of liquid electrolyte, the solid electrolyte could have the dissolved oxygen sensor be miniaturized. To prove the feasibility, the solid electrolyte with various proportions was t ested the impedance and the conductivity. With a DC power supply to input fixed voltage, a multimeter was utilized for measuring the electric current so that the impedance of the solid electrolyte with various proportions was cal culated. Furthermore, using a spi n coater to test the coating feasibility of the solid electro lyte with various proportions, the solidification time was evaluated. An appropriate proportion was sel ected for the following experiment. The test results were listed in Table 2, where t he proportion of 4：1 presented proper i mpedance and short solidification time and was able to be coated with a spin coater. When the mixture proportion was det ermined, the conductivity test was further preceded. W ith a DC power supply to input voltage, the solid electrolyte was tested with an LED. The electrolyte was first linked with the positive electrode and the negative electrode and t hen the LED bul b and the DC power supply. After appropriate voltage was input, the LED bulb was actu ally lit up, presenting that the electrolyte did work.

The solid electrolyte with the proportion of 4：1 was coated on the sensing electrode. In order to test the effect of thickness on t he dissolved oxygen chip sensor, different thicknesses of 5 *μm*, 10 *μm*, and 50 *μm* were coated on the solid electrolyte, which was pl aced in room temperature for 24 *hr* to naturally solidify the gelatinous electrolyte. The process of the solid electrolyte was then completed.

E. The Process of Permeability Layer

Both silicone rubber and cellulose acetate were applied as the permeability layers. After co mpleting the solidification of the gelatinous electrolyte, silicone rubber was evenly coated on the solid electrolyte, which was then placed in room temperature for 24 hr. W hen the silicone rubber was naturally solidified, the silicone rubber permeability layer was co mpleted, Fig. 2. Adding cellulose acetate to ethylene glycol diacetate with the weight proportion of 1：6, it was heated to 150℃ till cellu lose acetate was completed dissolved for coating. Then the solid electrolyte was placed in room temperature for 24 hr to naturally solidify the cellulose acetate. The cellulose acetate permeability layer was therefore completed, Fig. 3.

III. STEPS FOR EXPERIMENTAL MEASUREMENT

A. Arrangement of Experimental Environment

The experimental equipment contained electrochemistry analyzer (Potentiostat), magnetic stirrer (Stirrer / hot plate), commercial dissolved oxygen meter, and dissolved oxygen chip sensor. The arrangement of the experimental environment is shown in Fig. 4. The sensing electrode on the dissolved oxygen chip sensor was connected with a conducting wire, which was linked with an electrochemistry analyzer for measurements.

B. Steps for Experimental Measurement

1) Proceeding Cyclic Voltammetry with Different Dissolved Oxygen

A magnetic stirrer was set at 2 6℃ with the revolution of 750 *rpm* to maintain the fluidity of the solution in the beaker. Pumping air to the solution in the beaker for 20 *min*, the oxygen content of t he solution was sat urated. A commercial dissolved oxygen meter was u tilized for the reference of t he solution dissolved oxygen in the beaker. When the oxygen content was saturated, cyclic voltammetry, with the scanning range 1.2 *V*～-0.8 *V*(vs. Ag/AgCl) and the scanning speed 50 *mV/sec*, was proceeded for a Cyclic voltammogram. Sodium sulfite presented the effect of deoxidization that it was added to the solution in the beaker for deoxidizing the solution. The Cyclic voltammogram of the solution with different dissolved oxygen was furt her compared.

2) Test of Response Time

With the sensing potential -0.6 *V*(vs. Ag/AgCl), the solid electrolyte with various thicknesses was measured the response time with the permeability layers of silicone rubber and cellulose acetate. Pum ping the solution for 20 *min* to saturate the solution oxygen content and addi ng sodium sulfite to deoxidize the saturated solution, the response time was then recorded.

VI. RESULTS AND DISCUSSIONS

A. Cyclic Voltammogram with Different Concentration

In this study, silicon wafers were utilized as the substrate. With film deposition in the microelectromechanical system to develop the electrode of the dissolved oxygen chip sensor, the mixed solid electrolyte was coated on the electrode and the permeability layer was further coated on the solid electrolyte. The completed dissolved oxygen chip sensor was placed in the solution with different dissolved oxygen for C yclic voltammetry. The m easurements of t he dissolved oxygen with 8 *ppm*, 6 *ppm*, 4 *ppm*, 2 *ppm*, and 0 *ppm*.

B. Test of Response Electric Current Curve

In the cyclic v oltammogram, where the dissolved oxygen with 8 *ppm*, 6 *ppm*, 4 *ppm*, 2 *ppm*, and 0 *ppm* was measured, the oxidation/deoxidization potential -0.6 *V*(vs. Ag/AgCl) was selected to draw the calibration curves of the response current and the dissolved oxygen concentration, in which the sensitivity appeared 0.278 *μA/ppm* and R^2 0.9531, showed in Fig. 5.

C. Test of Response Time

With the sensing potential -0.6 *V*(vs. Ag/AgCl) to test the response time, the solution was pum ped for 20 *min* to reach dissolved oxygen saturati on, and sodium sulfite was added to the solid electrolyte with various thicknesses for

testing the response time with silicone rubber and cellulose acetate, shown in Table 3. With silicone rubber and cellulose acetate as the permeability layers, the 5 *μm*-thick solid electrolyte with silicone rubber presented the response time about 120 *sec*, and appeared about 15 sec with cellulose acetate. The 10 *μm*-thick solid electrolyte with silicone rubber as the permeability layer presented the response time around 150 *sec*, while it appeared about 23 *sec* with cellulose acetate as the permeability layer. The 50 *μm*-thick solid electrolyte with silicone rubber as the permeability layer showed the response time around 170 *sec*, while it revealed about 54 *sec* with cellulose acetate as the permeability layer. Figure 5 showed that sensitivity in water reached 0.278 *μA/ppm*, the monitored dissolved oxygen value ranged between 0~8 *ppm*, and R^2 was 0.9531.

V. CONCLUSION

This study applied single silicon wafers as the substrate so that the dissolved oxygen chip sensor could be easily miniaturized without the design of microchannel. Besides, the mixed solid electrolyte was utilized for the electrolyte as it was easily produced and appeared no risk of leakage. Both silicone rubber and cellulose acetate were used as the permeability layers for comparing the response time. Waters were utilized as the sample for monitoring the solution. In domestic and international literatures, the solution with higher ions, such as NaCl and KCl, was generally applied. The experimental results showed that the sensitivity in water reached 0.278 *μA/ppm*, the monitored dissolved oxygen value ranged between 0~8 *ppm*, and R^2 was 0.9531. With silicone rubber as the permeability layer, the response time was around 120 *sec*, while it was about 15 *sec* with cellulose acetate as the permeability layer.

'''ACKNOWLEDGEMENT

REFERENCES

[1]. Fisheries Agency, Council of Agriculture, Executive Yuan, Taiwan, *2009 Taiwan Fisheries Yearbook*, (2010).

[2]. H.-C. Chiang, *Water quality analysis*, San Ming Book Company, Taiwan, (2001).

[3]. C.-H. Yu, *Research and development of low-cost dissolved oxygen sensor*, M. S. Thesis (in Chinese), National Taiwan University, Taiwan, (2005).

[4]. 酒井信, "膜を通した酸素の水にまる吸收速度", 北海道大學水產彙報, 43 (1992), 193-201.

[5]. L.-S. Lee, *Aquaculture*, Chien Cheng Publishing Company, Taiwan, (2008) 72.

[6]. D. R. Raible, "*Survival and growth rate of channel catfish as a function of dissolved-oxygen concentration*", Water resources research Center Publication, Univ. Ark. Fayetteville, 33 (1975) 35.

[7]. B. A. Simco, "The reuse of water in commercial raising of catfish: phase two", Univ. Tenn. Water Res. Ctr. Res. Rep. 52 (1976) 66.

TABLE 1 Adaptation of fish in the water with different dissolved oxygen concentration.

Dissolved oxygen concentration (*ppm*)	status
1	dead
2	danger
3~4	warning
5	safe
6~9	**GOOD**
10~13	safe

TABLE 2 The conductivity test results for different mixture proportion between gelation and potassium nitride.

Mixture proportion	Voltage (*V*)	Current (*mA*)	Impedance (*KΩ*)	Solidification time	Created by spin coating
2：1	1	0.026	38.46	<1 day	No (Too dense)
	2	1.03	1.94		
	3	5.28	0.56		
4：1	1	0.021	47.61	1 day	Yes
	2	1.65	1.21		
	3	5.23	0.57		
8：1	1	0.017	58.82	>3 days	Yes
	2	3.62	0.55		
	3	5.33	0.56		

TABLE 3 The response time for different solid electrolyte thickness and gas-permeable membrane design.

Working electrode material	Working electrode area	Gas-permeable membrane	Solid electrolyte thickness	90% response time
Au	20 *mm²*	Silicone rubber	5 *μm*	120 s
			10 *μm*	150 s
			50 *μm*	170 s
		Cellulose acetate	5 *μm*	15 s
			10 *μm*	23 s
			50 *μm*	54 s

(1) Cr/Au deposition
(2) Pattern transfer with Mask#1
(3) Au electrode creation
(4) Pattern transfer with Mask#2
(5) Ag electrode deposition
(6) lift-off PR
(7) Pattern transfer with Mask#3
(8) Cr etching and PR removing
(9) Pattern transfer Mask #4
(10) AgCl creation
(11) Solid electrolyte deposition
(12) Permeability layer deposition

Silicon Cr Au Ag/AgCl Solid electrolyte
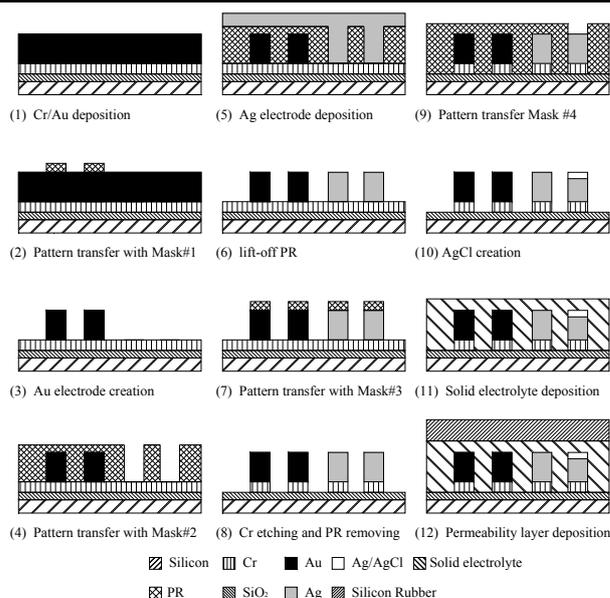PR SiO₂ Ag Silicon Rubber
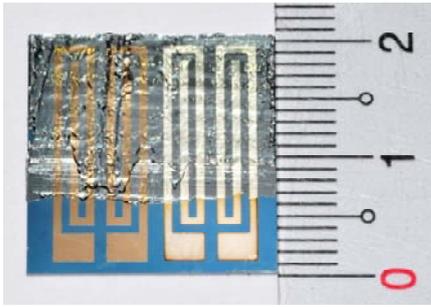
Fig. 1 Process flow for dissolved oxygen chip sensor.

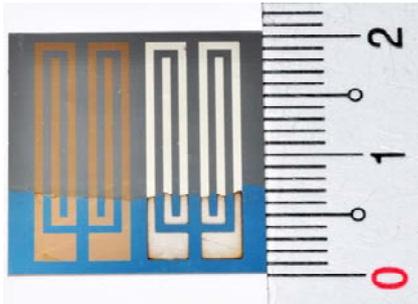Fig. 2 The dissolved chip sensor with silicon rubber permeability layer coating.

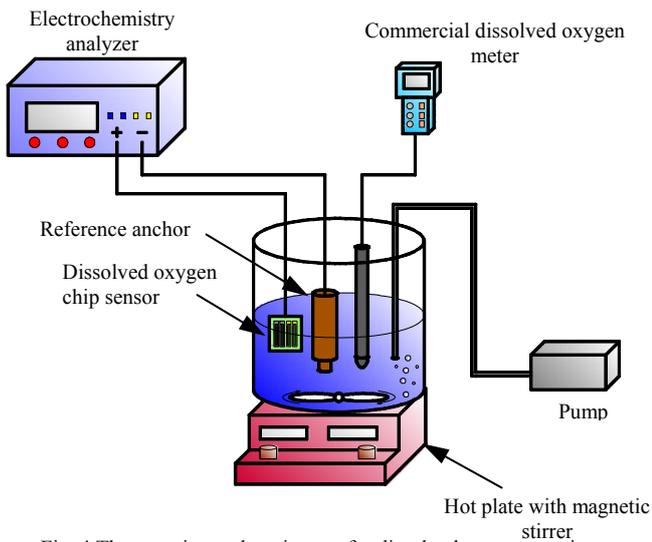Fig. 3 The dissolved chip sensor with cellulose acetate permeability layer coating.

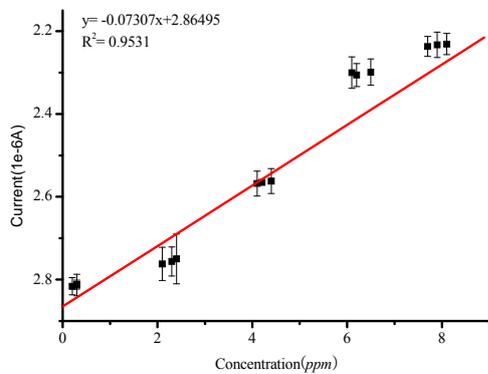Fig. 4 The experimental equipment for dissolved oxygen sensing.

Fig. 5 The relation between the response current and dissolved oxygen concentration.